High rejection, Self-packaged Lowpass Filter using Multilayer Liquid Crystal Polymer Technology

Francisco Cervera, *Student Member, IEEE,* and Jiasheng Hong, *Fellow, IEEE*

***Abstract*—A compact lowpass filter based on the principle of destructive interference is proposed and analysed, followed by an improved design demonstrating very high rejection levels better than 40 dB over a wide frequency span. Both filters, fabricated using liquid crystal polymer (LCP) multilayer techniques, are self-packaged, with small footprint and profile, and also very light weight. Simulation and measured results are presented, showing good agreement.**

***Index Terms*—Lowpass filters, clean-up, liquid crystal polymer, microwave filters, self-packaged filters, high rejection, destructive interference.**

I. Introduction

LOW pass filters (LPF) are a key element in order to eliminate spurious resonances and unwanted passbands originated by intermodulation or the intrinsic nature of distributed resonators. Often they are chained to some other filters and, hence, a very low insertion loss (IL) over a desired passband, together with a deep stopband rejection, is commonly required for practical applications.

One of the main concerns when designing a LPF is the suppression of higher harmonics and providing a wide stopband. Extensive research has been carried towards this aim using different approaches. A popular approach is cascading successive LPFs with different cutoff frequencies [1]–[5]. A different method is employed in [6]–[10], where several transmission zeroes (TZs) are inserted in the stopband by including resonating elements, cancelling spurious harmonics. Furthermore, defected ground structures (DGS) are also investigated [11]–[13] to produce a wide stopband. However, the latter have the inconvenience of breaking the ground plane, and potentially increasing the radiation of the filter.

Even though the aforementioned LPFs provide a wide stopband, most of them are in the region of 20 dB for the rejection level, which would not meet the requirements for a more demanding clean-up filter. Work reported in [5], [13], [14] achieves deeper rejection levels, being the latter highly demanding in terms of fabrication technology.

Also key to a LPF is the selectivity, or how short in frequency is the transition from the passband to the stopband. Previously referenced work provide very sharp transitions [5]–[8], [10], [12], [15], at the cost of lower performance on some other aspects like return loss (RL), rejection level, or stopband bandwidth. Despite being desirable, a sharp cutoff is not crucial in a clean-up filter.

Francisco Cervera and Jiasheng Hong are with the Institute of Signal, Sensors, and Systems (ISSS), School of Engineering and Physical Sciences, Heriot-Watt University, Edinburgh, EH14 4AS, U.K. Email: fc88@hw.ac.uk, J.Hong@hw.ac.uk.

This work was supported in part by a UK EPSRC Industrial CASE Award in association with BSC Filters Ltd, UK.

Manuscript received March xx, 2015.

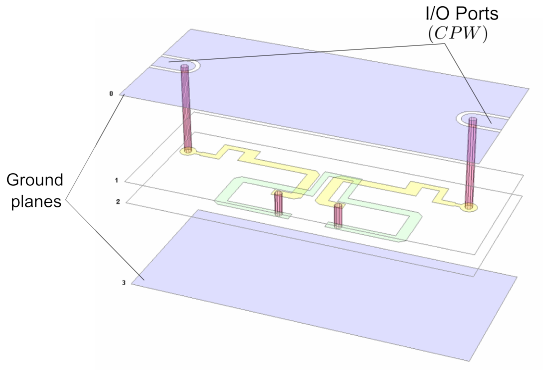

Fig. 1. Proposed self-packaged low pass filter structure (see Fig. 16 for a 2D representation)

Furthermore, a packaged filter with small size and weight is desired for a highly integrated system to minimize unwanted cross talking as well as to accommodate the system restraint in size/weight. As such, the aim of this work is to design a compact, inexpensive, self-packaged LPF as shown in Fig. 1, focusing on the rejection levels of the stopband while maintaining a low IL. For this purpose, a structure based on the principle of destructive interference [1], [3], [16] is applied, and a second identical structure is cascaded in order to increase the rejection levels.

The basic unit for the low pass is a structure with two broadside coupled lines and an extra line (*loop line*) connecting alternate ends of the coupled lines section (Fig. 2a). This kind of structure has been investigated as an impedance transformer [17] replacing the loop line for a two-section stepped impedance line. Additionally, a similar structure has been reported in [3], using different outputs from the coupled lines. Both structures are based on the principle of destructive interference and are capable of producing up to $R + 1$ transmission zeros (TZ) [3], being R the electrical length ratio between the loop line (θ_L) and the coupled section (θ_C).

In this work, a modified structure is investigated where the loop line is replaced by a three-section stepped impedance line, with two of the sections being equal in length and impedance (Fig. 2b). It will also be shown how, under certain conditions, the same number of TZ's can be excited with lower values of R. Additionally, the use of multilayer technology, allows for the use of broadside-coupled lines, rather than egde-coupled lines, leading to higher coupling ratios, as well as different

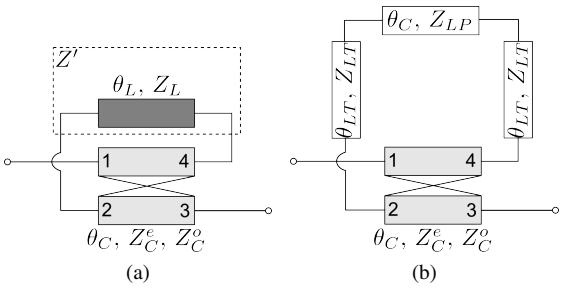

Fig. 2. Transmission line model (a) Uniform line (b) Stepped-impedance line

layouts than those achieved with single-layer configurations.

The rest of this article is organised as follows: Section II covers the theory and concepts of the structure for a generic loop line. Sections III and IV cover the analysis of the structure when the generic line is replaced by an uniform-line (Fig. 2a) and a stepped-impedance line (Fig. 2b), respectively. Two design examples are discussed in Sections VII and VIII, finalising with conclusions in Section IX.

II. Generic loop structure

The structure is based on a pair of broadside coupled-lines plus an additional section joining alternate ends (Fig. 2). The coupled-lines can be described in terms of its characteristic impedance (Z_C), coupling coefficient (k), and electrical length (θ_C) as follows:

$$Z_C = \sqrt{Z_C^e Z_C^o} \tag{1a}$$

$$k = \frac{Z_C^e - Z_C^o}{Z_C^e + Z_C^o} \tag{1b}$$

where Z_C^e and Z_C^o are the even- and odd-mode impedances, respectively. The additional section producing the interference is defined as a two port network by its Z-parameters (Z') (see dashed boxes in Fig. 2). Given this structure is reciprocal and symmetrical ($Z_{11} = Z_{22}$ and $Z_{12} = Z_{21}$), and lossless, non-dispersive propagation, the Z-parameters of the complete 2-port structure are derived as:

$$\begin{aligned} Z_{11} = Z_{22} &= -jZ_C\frac{\alpha_{11}+\beta_{11}}{\Delta} \\ \alpha_{11} &= q(Z_{11}'^2 - Z_{12}'^2 + Z_C^2)\sin\theta_C\cos\theta_C \\ \beta_{11} &= jZ_C Z_{11}'[(1+q^2)\sin^2\theta_C - q^2] \end{aligned} \tag{2}$$

$$\begin{aligned} Z_{12} = Z_{21} &= -jZ_C\frac{\alpha_{12}+\beta_{12}}{\Delta} \\ \alpha_{12} &= qk(Z_{11}'^2 - Z_{12}'^2 - Z_C^2)\sin\theta_C \\ \beta_{12} &= jZ_C Z_{12}'(k^2\sin^2\theta_C - q^2) \end{aligned} \tag{3}$$

$$\begin{aligned} \Delta = &[(Z_{11}'^2 - Z_{12}'^2)q^2 + Z_C^2]\sin^2\theta_C - Z_C^2 q^2 \\ &+ j2qZ_C(Z_{12}'k - Z_{11}'\cos\theta_C)\sin\theta_C \end{aligned}$$

where $q = \sqrt{1-k^2}$. The scattering parameters (S-Parameters) can be obtained from the Z-parameters using the well known formulas:

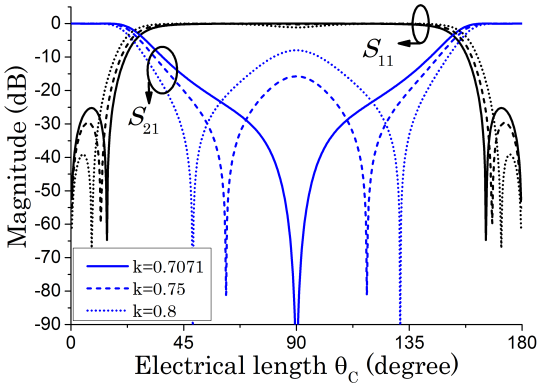

Fig. 3. S-Parameters when $Z_L = Z_C$ for different values of k. ($R = 3$, $Z_L = Z_C = 30\ \Omega$, $Z_0 = 50\ \Omega$)

$$S_{11} = \frac{Z_{11}^2 - Z_0^2 - Z_{21}^2}{(Z_{11}+Z_0)^2 - Z_{21}^2} \tag{4a}$$

$$S_{21} = \frac{2Z_{21}Z_0}{(Z_{11}+Z_0)^2 - Z_{21}^2} \tag{4b}$$

where Z_0 is the reference impedance.

III. Uniform loop line

Following the discussion from the previous section, a uniform transmission line is used as a loop-line (Fig. 2a), defined by its Z-parameters:

$$\begin{aligned} Z_{11}' = Z_{22}' &= -jZ_L\cot(\theta_L) \\ Z_{12}' = Z_{21}' &= -jZ_L\csc(\theta_L) \end{aligned} \tag{5}$$

where θ_L is the electrical length of the line and Z_L, its characteristic impedance.

A. Transmission zeros

From (4b), the condition for a transmission zero is $Z_{21} = 0$. Applying this to (3), and including (5), the condition for the transmission zeros (TZ) is calculated as:

$$sin(R\theta_C) = \frac{Z_L Z_C}{(Z_L^2 - Z_C^2)\frac{q}{k}}\frac{(\frac{q}{k})^2 - sin^2\theta_C}{sin\theta_C} \tag{6}$$

where $R = \theta_L/\theta_C$ is the ratio between the lengths of the loop-line and the pair of coupled-lines. It is direct to show the symmetry of the response for integer values of R around $\theta_C = \pi$. Moreover, if R is odd, the response will also be symmetric around $\theta_C = \pi/2$.

From (6) an interesting property is derived: if $Z_L = Z_C$, i.e. matching the line impedance to the coupled-lines characteristic impedance, two TZs are generated in $\theta_C(0,\pi)$ and their position depends exclusively on k, rather than R, (Fig. 3) as demonstrated in:

$$Z_L = Z_C \implies \theta_{TZ} = \arcsin\frac{q}{k} = \arcsin\frac{\sqrt{1-k^2}}{k} \tag{7}$$

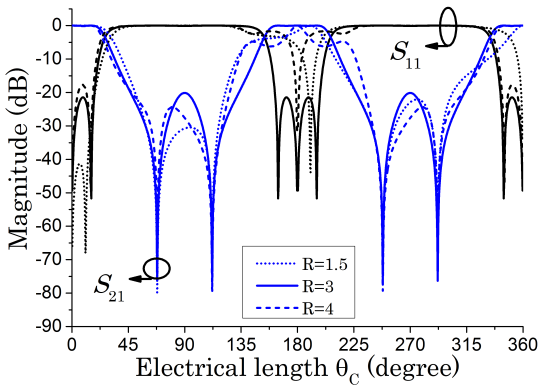

Fig. 4. S-Parameters when $Z_L = Z_C$ for several length ratios. ($Z_L = Z_C = 27.82\ \Omega$, $k = 0.733$, $Z_0 = 50\ \Omega$)

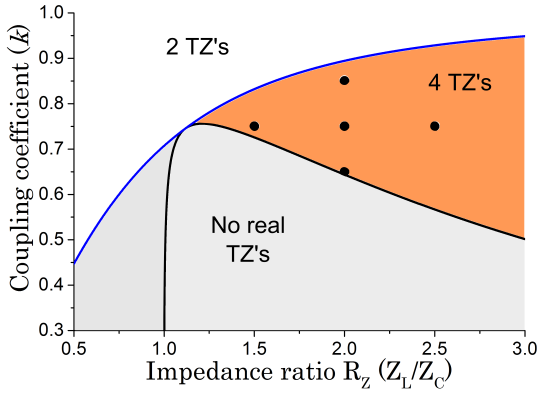

Fig. 5. Different regions depending on the number of TZ's. (•) in the 4-TZ's region correspond to plots in Fig. 6 and Fig. 7.

This pair of TZs are real for $k \geq 1/\sqrt{2}$. The high value of k required to fulfil this condition makes this structure more suitable for broadside coupled lines using multilayer techniques, where higher coupling coefficients can be obtained. Since the position of the TZs is not affected by the length of the loop line, this structure has possible applications as a phase-shifter. A representation of the aforementioned property is depicted in Fig. 4. Different symmetries depending on the value of R can also be appreciated.

If the value of R is fixed to 3, a compact structure with up to four TZ's is obtained. From this point and for the rest of the paper, $R = 3$ is assumed unless stated. The condition for TZ's in such conditions can be obtained from (6) as follows:

$$4\sin^4\theta_C - (3 + Z_x\frac{k}{q})\sin^2\theta_C + Z_x\frac{q}{k} = 0 \tag{8}$$

$$Z_x = \frac{Z_L Z_C}{Z_L^2 - Z_C^2} = \frac{R_Z}{R_Z^2 - 1}$$

with $R_Z = Z_L/Z_C$ being the ratio between the line and the coupled-lines characteristic impedances. By solving (8) for θ_C, the location of the four TZ's is found as:

$$\theta_{TZ} = \sin^{-1}\left(\pm\sqrt{\frac{3 + Z_x\frac{k}{q} \pm \sqrt{(3 + Z_x\frac{k}{q})^2 - 16Z_x\frac{q}{k}}}{8}}\right) \tag{9}$$

The position of the TZ's are determined by k and R_Z, and depending on their values, they could be real or imaginary. Attending to this, and considering the number of TZ's within the $0 < \theta_C < \pi$ range, three different working regions are found (Fig. 5):

- 4-TZ region, when

$$\begin{aligned} k &< \frac{R_Z}{\sqrt{R_Z^2 + 1}} \\ (3 + Z_x\frac{k}{q})^2 &> 16Z_x\frac{q}{k} \\ R_Z &> \frac{\sqrt{5}}{2} \end{aligned} \tag{10}$$

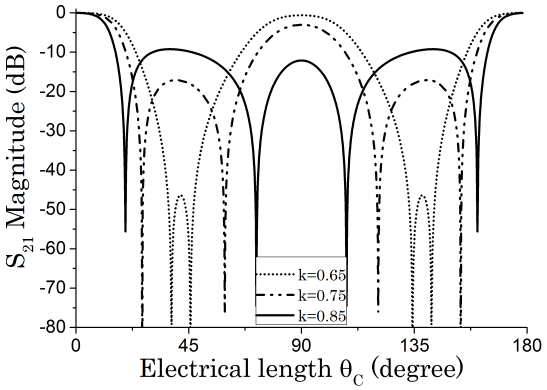

Fig. 6. TZ variation for different values of k (Z_C=30 Ω, $R_Z = 2$)

- 2-TZ region, when

$$k > \frac{R_Z}{\sqrt{R_Z^2 + 1}} \tag{11}$$

- No real TZs, if the previous conditions are not met.

Note how the location of TZ's is independent from Z_C. However, variations in this parameter would affect the rejection levels. Lower values of Z_C would increase the rejection between the first and last pair of TZ's, while reducing it between the second and third TZ.

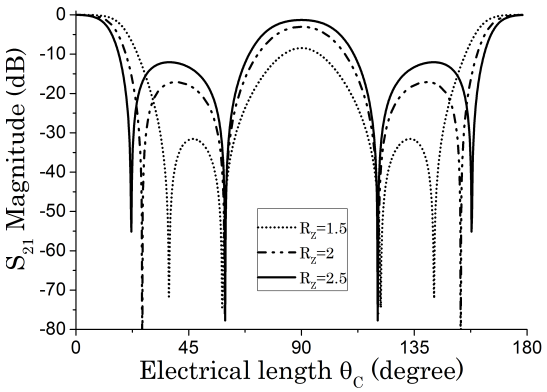

Fig. 7. TZ variation for different values of R_Z ($k = 0.75, Z_C = 30\ \Omega$)

In order to obtain a wide and deep rejection band, the 4 TZ's region is the most interesting one. Several pairs of R_Z and k within it are plotted in Fig. 6 and Fig. 7 (also marked on Fig. 5). It can be appreciated how variations of k would equally affect all the TZ's, while variations of R_Z would mainly affect the first and fourth TZ, having a negligible effect on the inner pair of TZ's. As a rule of thumb, higher values of k increase the stopband width and selectivity, reducing the rejection level.

B. Transmission poles

From (4a), the transmission pole (TP) condition is:

$$Z_{11}^2 - Z_{21}^2 = Z_0^2 \tag{12}$$

This expression can be rewritten as:

$$\frac{Z_0^2}{Z_C^2} = \frac{(\alpha_{11}+\beta_{11})^2 - (\alpha_{12}+\beta_{12})^2}{\Delta} \tag{13}$$

The right hand side of the expression only depends on θ_C and R_Z (assuming R_Z independent from Z_C), so the TP condition is dominated by Z_C. By using algebraic transformations, it can be demonstrated that for values of θ_C in the passbands, a maximum of two poles can be obtained, with one of them located at $\theta_C = 0$. Reducing Z_C will approximate the second TP to the cutoff frequency. Taking the limit when $Z_C = 0$, TP's are located at the roots of Δ. On the other end, taking the limit when $Z_C = \infty$, makes the two TP to meet at $\theta_C = 0$.

C. Cutoff frequency

In order to determine the 3 dB cutoff frequency (θ_{3dB}), k, R_Z and Z_C are the key parameters. Fig. 8 show different design curves, based on numerical solutions of (4b) for 3 dB, for these parameters. According to the figures, both k and Z_C have similar effects on the cutoff frequency, when working on the 4-TZ's region, i.e. $R_Z > \sqrt{5}/2$. Moreover, they both can be combined to obtain the desired cutoff.

As R is fixed to 3, the response of the filter is symmetric around $\theta_C = \pi/2$. With this, we can determine the stopband bandwidth (BW) depending on f_C as:

$$FBW = \frac{\pi - 2\theta_{3dB}}{\pi/2} \tag{14}$$

Or, as a function of f_C, as:

$$BW(f_C) = (\frac{\pi}{\theta_{3dB}} - 1) f_C \tag{15}$$

IV. Stepped-impedance loop structure

Likewise the previous section, the uniform loop-line is now replaced by a three-section impedance line (Fig. 2b). For simplicity, the length of the middle section is equal to the length of the coupled lines ($\theta_2 = \theta_C$). The other two sections have the same length (θ_1). Furthermore, we can define the impedance ratio of the loop line as:

$$R_S = \frac{Z_2}{Z_1} \tag{16}$$

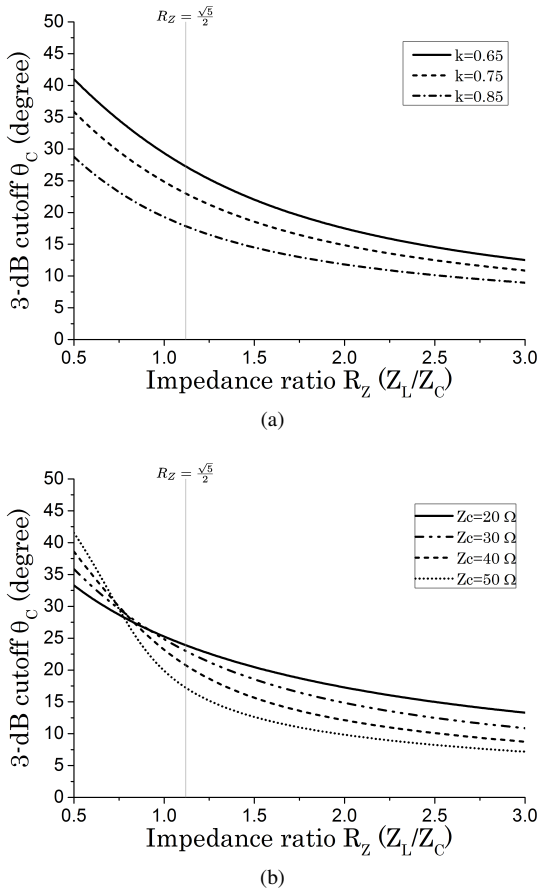

Fig. 8. 3-dB cutoff frequency (a) for different values of k ($Z_C = 30\ \Omega$) (b) for different values of Z_C ($k = 0.75$)

where Z_2 is the impedance of the line section parallel to the coupled lines, and Z_1 the impedance of the remaining two sections. Following the convention for the uniform-line case, R_Z is defined now as Z_1/Z_C. In this way, the response from the coupled-line loop unit can be initially determined by the coupled lines parameters (θ_C, Z_C, k) and the loop line parameters (θ_1, R_Z, R_S).

The modification is particularly interesting when the length ratio (R) is fixed to 3, i.e. fixing $\theta_1 = \theta_2 = \theta_C$, as will be discussed in this section. Under this conditions, the Z-parameters for the loop line are:

$$\begin{aligned} Z'_{11} = Z'_{22} = \\ -jZ_1 \cot\theta_C \frac{(R_S+1)^2 \sin^2\theta_C - R_S}{(R_S+1)^2 \sin^2\theta_C - 2R_S - 1} \\ Z'_{12} = Z'_{21} = \\ jZ_1 \csc\theta_C \frac{R_S}{(R_S+1)^2 \sin^2\theta_C - 2R_S - 1} \end{aligned} \tag{17}$$

A. Transmission zeros

As previously discussed, the structure is capable of producing up to four TZ's in the stopband and the response will be symmetric. The advantage introduced by this configuration is a better control over the response in the stopband as the position of the two inner TZ's can be adjusted with R_S without

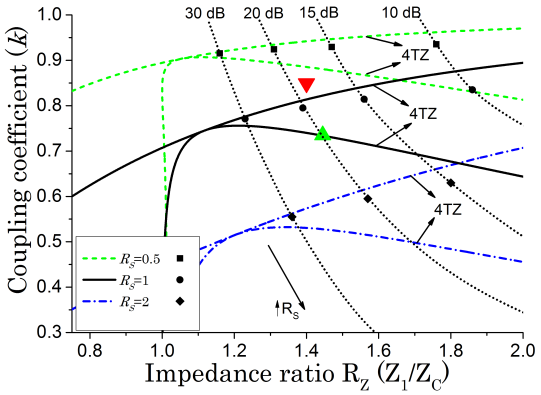

Fig. 9. TZ regions for different values of R_S. Dotted lines correspond to equal-ripple stopband with the labelled rejection for $Z_C = 28\ \Omega$. ($\bigtriangledown$) Section VII design ($R_S = 0.83, Z_C = 20.97\ \Omega$) ($\bigtriangleup$) Section VIII design ($R_S = 1.44, Z_C = 28.14\ \Omega$)

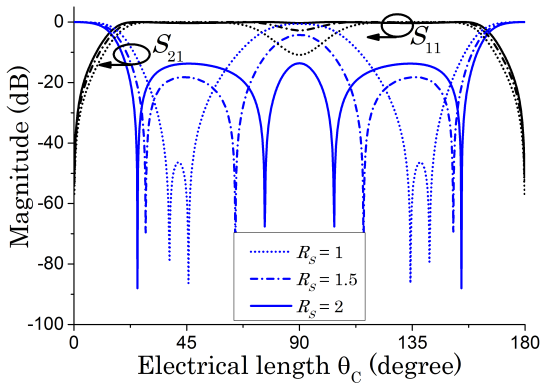

Fig. 10. S-Parameters for different values of R_S ($k = 0.65, Z_C = 30\ \Omega, R_Z = 2$)

having too much impact on the outer ones, thus enabling the possibility of obtaining an equal-ripple stopband (Fig. 10).

Following the procedure described in the previous section, replacing Z' for the stepped-line in (3), and making $Z_{21} = 0$, the condition for TZ is found as:

$$\frac{(R_S+1)^2}{R_S}\sin^4\theta_C - \left(Z_x\frac{k}{q} + 2 + \frac{Z_x}{Z_y}\right)\sin^2\theta_C + Z_x\frac{q}{k} = 0 \quad (18)$$

$$Z_y = \frac{Z_2 Z_C}{Z_2^2 - Z_C^2} = \frac{R_Z R_S}{R_Z^2 R_S^2 - 1}$$

As in the previous section, the different working regions are plotted in Fig. 9. It can be observed how they are similar to the uniform-line case, but the position is shifted over k. This effect suggests that similar responses can be obtained with lower k when this is compensated with higher values of R_S. Moreover, variations of R_S for fixed values of k, Z_C, and R_Z are depicted in Fig. 10. Further variations of k and R_Z have a similar effect as in the uniform line case. As an example, design values for the fabricated filters are marked. Note how the effect of R_S makes the design in Section VII to have 4-TZ's, instead of the expected two in the uniform-line case.

B. Transmission poles

Using a similar derivation as in Section III-B, the right hand side of (13) in the case of a stepped-impedance line, depends on θ_C, R_Z, and R_S. The position of the second TP may be controlled by Z_C/Z_0 ratio, ranging from $Z_C = 0$ to the first root of Δ.

C. Cutoff frequency

In the case of an uniform-line, the cutoff frequency (f_C) could be determined based on the (k, Z_C, R_Z) set of parameters. For a stepped-impedance line, R_S also has to be included in this group. Variations of this parameter have a similar effect to variations of k.

From (2) and (3) it can be found that the most relevant term is $Z_{11}'^2 - Z_{12}'^2$. In order to establish a relationship between the cutoff frequencies in the uniform- and the stepped-line cases the mentioned term may be matched at cutoff frequency, obtaining the following relationship:

$$\frac{R_{Zunif}^2}{R_{Zstep}^2} = \frac{(R_S+1)^2\sin\theta_0^2 - 2R_S - R_S^2}{(R_S+1)^2\sin\theta_0^2 - 2R_S - 1} \quad (19)$$

where θ_0 is the electrical length of the coupled lines (θ_C), at the matched cutoff frequency, R_{Zunif} and R_{Zstep} are the R_Z for the uniform- and stepped-line cases, and R_S is the impedance ratio of the stepped-line.

Since we are matching both cases for the pass-band, θ_0 would be a small value. Therefore, (19) can be simplified to:

$$\frac{R_{Zunif}^2}{R_{Zstep}^2} = \frac{2R_S + R_S^2}{2R_S + 1} \quad (20)$$

By establishing this relationship, the return loss for the stepped-line can match that of the uniform-line for a given pair (R_Z, R_S). As such, Fig. 8 can be used for estimating the cutoff frequency.

D. Equal ripple

By modifying R_S, a wide stop-band with equal ripple can be obtained. The condition for equal-ripple can be determined by equating the values of S_{21} in the cases of $\theta = \pi/2$ and $\theta = \theta_M$, being θ_M the frequency between the first two TZ's with the maximum value of S_{21}, defined as:

$$\frac{\partial|S_{21}|}{\partial\theta} = 0 \quad (21)$$

$$|S_{21}(\theta = \frac{\pi}{2})| = |S_{21}(\theta = \theta_M)| \quad (22)$$

This expression needs to be solved numerically, as a simple solution is not available. However, as a rule of thumb, increasing R_S will bring the pair of inner TZ's closer to $\theta_C = \pi/2$, hence reducing the transmission power at the center frequency (f_0). Adjusting R_S will lead to equal ripple.

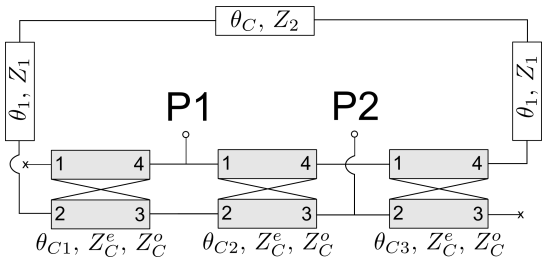

Fig. 11. Modified loop-line structure ($\theta_C = \theta_{C1} + \theta_{C2} + \theta_{C3}$). P1 and P2 represent the I/O ports

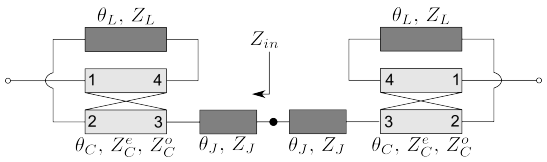

Fig. 12. Cascaded model (uniform line case)

E. Footprint reduction

Initially, the structures depicted in Fig. 2 can be physically realised by feeding the coupled lines from the side edges. However, if the tapping point of the feeding lines are shifted (Fig. 11), equivalent responses can be obtained with a reduced length of the loop line.

Shifting the feeding lines reduces the effective length of the coupled line section, therefore, in order to achieve the same f_C, the length of the coupled-lines section will have to be increased. However, the reduction of the length of the loop-line would be more significant, obtaining an overall size reduction when combined. The pair of coupled lines act as a half-wavelength resonator, so the limitation for increasing the length comes when the resonant mode is within the stop-band. Footprint reduction will be demonstrated with an example in Section VIII.

F. Cascading

Even though the stopband achieved with a single unit can be in the region of 20-30dB for a reasonable bandwidth, this is not enough for many practical applications. One way of increasing the level of rejection without affecting the BW would be cascading to filters with identical characteristics. In this case, the order of the filter is doubled, and so is the level of rejection, while keeping the position of the TZ's intact.

When cascading two filters together with a section of transmission line, some resonances may appear. These resonances have two different origins. First, matching of the input impedance ($Z_{in} = 0$), looking into the filter from the interconnection point (Fig. 12), and second, the loop-structure self-resonance, located at $\theta_C = \pi/2$ when $R = 3$.

The proposed idea for avoiding these resonances is matching them with the TZs. In other words, making $Z_{in} = 0$ at the frequencies with TZ (θ_{TZ}). Z_{in} is defined in terms of Z-parameters as:

$$Z_{in} = Z_{11} - \frac{Z_{12}Z_{21}}{Z_{11} - Z_L} \tag{23}$$

Since $Z_{12} = Z_{21} = 0$ at TZ, it is immediate to demonstrate:

$$Z_{in}(\theta_{TZ}) = Z_{11}(\theta_{TZ}) = Z_{22}(\theta_{TZ}) \tag{24}$$

The simplest form of matching network for this purpose is a uniform transmission line of a determined length (θ_J) and characteristic impedance (Z_J). Designing these parameters accordingly, at least the first TZ can be matched by using:

$$\theta_J = \frac{\pi/2}{\theta_{TZ1}} \arctan \frac{Z_{in}(\theta_{TZ1})}{Z_J} \tag{25}$$

The rest of possible resonances have to be matched by optimizing the structure.

V. Design method

Even though different parameters involved in the design are closely related and influence each other, the following design process may be used as a guide. It comprises five steps:

- Determine required cutoff frequency in terms of θ_C, i.e. θ_{3dB}, that fulfills the requirements for FBW, and find l_C using:

$$f(\theta)(\text{GHz}) = \frac{300}{l_C(\text{mm})\sqrt{\epsilon_{re}}} \frac{\theta(\text{rad})}{2\pi} \tag{26}$$

- Design coupled lines (k, Z_C) and R_Z for the uniform-line case, i.e. R_{Zunif}, that provides the required θ_{3dB}, with the help of Fig. 8.
- Using Fig. 9 as a reference, estimate a new R_Z, i.e. R_{Zstep}, that meet the requirements for stopband rejection for the chosen k.
- Calculate R_S from (19) for the previously found R_{Zunif} and R_{Zstep}.
- Check the design parameters meet the conditions to work in the 4-TZs region and fulfill the requirements for bandwidth and rejection. If any of these restrictions is not met, the coupled lines must be re-designed.

VI. Packaging

Following the work carried in [18], the filter structure is enclosed within two ground planes in a stripline configuration. Additionally, a conductive paste is applied in the surrounding walls in order to achieve a full electromagnetic shielding.

Filters are connected to the outer environment by means of a coplanar waveguide (CPW), printed on one of the ground planes, and via transition (Fig. 1). In order to adapt the designs to this packaging, feed lines may need to be extended with lines matching port impedances, so the filter accommodates to the CPW layout (Fig. 16c).

This kind of packaging allows easy interconnection of the device to a hosting board in a flip-chip manner, as well as allowing easy matching of the input impedance by modifying the width and gap in the CPW.

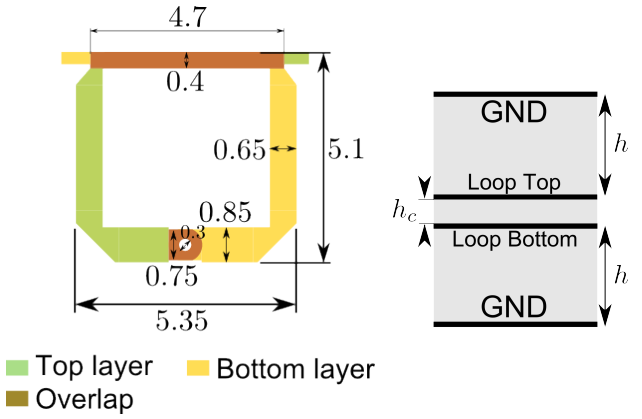

(a) (b)

Fig. 13. Design details (a) Top view (dimensions in mm) (b) Layer distribution ($h_c = 25\mu m$, $h = 0.2mm$)

VII. Design Example

In order to demonstrate the theory previously discussed, a design example will be introduced in this section. Requirements for this filter are:

- Cutoff frequency: 2GHz
- Stopband up to $9f_C$, equivalent to 160% fractional bandwidth (FBW)
- Equal ripple with 20dB rejection

Following the design method previously described, at the first step, and from (14), $\theta_{3dB} = 18^o$ for a 160% FBW is found. With this value, l_C that maps θ_{3dB} to 2 GHz, from (26), is 4.33 mm. Each of the three sections of the stepped-impedance loop-line have the same length as the coupled lines ($\theta_1 = \theta_2 = \theta_C$).

In the second step, coupled-lines parameters have to be designed, as well as the corresponding R_Z. In this case, the coupler is designed with $Z_C = 20.97\ \Omega$ and $k = 0.849$. With these values, R_Z that provides the required cutoff is 1.32.

Next step is to find a R_Z (Fig. 9) that provides equal-ripple and required rejection for the chosen k and Z_C. Note that equal-ripple curves in Fig. 9 are based on a $Z_C = 28\ \Omega$, so it can only be used as an approximation. Different values of Z_C would shift these curves slightly while keeping a similar tendency. The required value for R_{Zstep} is 1.4. By replacing it and R_{Zunif} in (20), $R_S = 0.83$ is obtained.

With the help of a EM simulator, some parameters are tuned to match the requirements. Final design values are plotted in Fig. 13. EM simulation results are plotted against the ideal model in Fig. 14. Mismatches, mainly in the fourth TZ, are produced by the corners in the loop-line, which are not included in the theoretical model. Spurious coupling and the via transition also contribute to the mismatch.

Measured results are plotted against EM simulation in Fig. 15, including the packaging. Even though they show a good correlation, some differences are found. These are due to fabrication tolerances, i.e. substrate thickness and etching. In order to achieve the tight coupling required, the coupled-lines are etched on a 25-μm-thick film (Fig. 13b). Its thinness magnifies the error introduced by misalignment and over-compression, explaining the mismatch in the results.

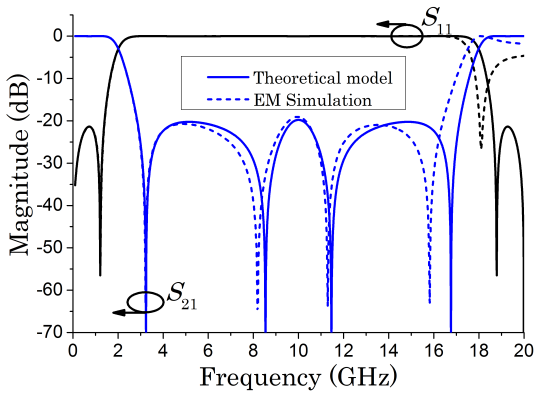

Fig. 14. Theoretical model vs. EM simulation ($\epsilon_r = 3$)

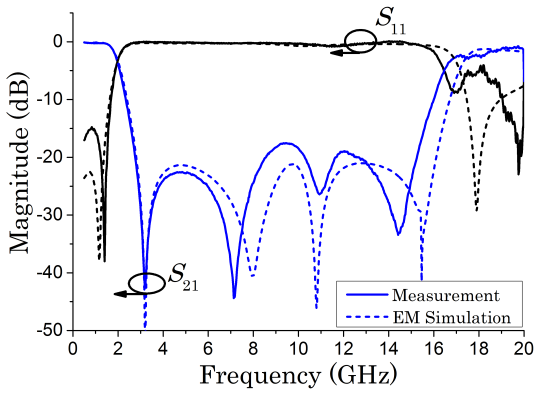

Fig. 15. Measured results vs. EM simulation, including packaging ($\epsilon_r = 3$).

VIII. Improved Rejection Filter Design

In this design we aim at designing a low-pass filter with improved rejection. Initial requirements are:

- Cutoff frequency: 3 GHz
- Stopband up to 8 f_C, equivalent to 155% fractional bandwidth (FBW)
- Equal ripple with, at least, 40 dB rejection

Such requirements cannot be fulfilled by a single loop structure. Instead, two of them with identical parameters are cascaded. As cascading two identical filters doubles the rejection level, each of these filters need to be designed for a 20 dB rejection, while keeping the rest of requirements.

A. Basic cell

Initial design is based on the procedure described in Section V. For a 155% FBW, the required $\theta_{3dB} = 20^o$, resulting in $l_C = 3.21$ mm. Coupled lines are designed with $Z_C = 28.14$ and $k = 0.734$, and the R_Z that provides the required cutoff (Fig. 8) is 1.56. Furthermore, values for obtaining a 20 dB equal-ripple in the stopband are $R_Z = 1.44$ and $R_S = 1.27$ (Fig. 9).

B. Footprint reduction

Based on optimization, the new values for the impedance ratios are $R_Z = 1.26$ and $R_S = 1.22$, and $\theta_{C1} = 10^o$. Thus,

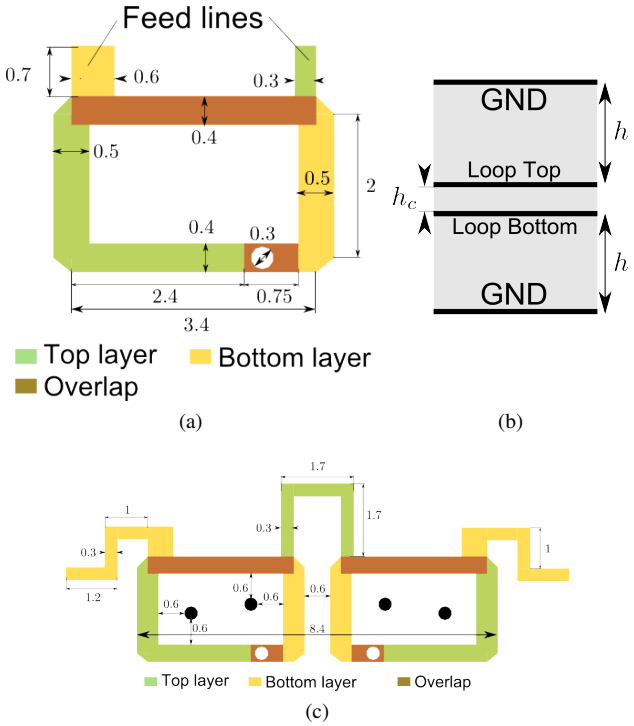

Fig. 16. Basic unit design details (a) Top view (dimensions in mm) (b) Layer distribution ($h_c = 50\mu m$, $h = 0.2mm$) (c) Final layout. Ground vias in black.

the length of the coupled lines is increased by 22%, being the new $l_C = 3.92$ mm. With these values, a similar response with the same f_C is obtained, as well as same rejection levels, with slightly reduced stopband width. These modifications lead to a 25% footprint reduction.

C. Cascading

The basic unit was designed for a 3 GHz cutoff frequency. This will need to be adjusted for a -1.5 dB, 3 GHz so the cascaded filter results in a 3 GHz at -3 dB. Therefore, l_C needs to be adjusted to 3.42 mm.

As discussed in previous sections, the two filtering units are connected by a uniform transmission line. The length and impedance of this line is designed to match Z_{in} at the first TZ. At this frequency, $Z_{in}(\theta_{TZ1}) = -j22.4\ \Omega$. By fixing $Z_J = 50\ \Omega$ and using (7), the matching value of θ_J is 54^o.

In order to match the rest of the Z_{in} singularities with the remaining three TZs, two parameters are optimized: the width of the via patch, and its shifting from the center of the line section parallel to the coupled lines.

Finally, the feed lines are designed to optimize the return loss, following the discussion in Section III-B with an impedance of 32 Ω. The impedance of the feed lines relates to Z_0 (13).

Additionally, an optimization process is carried with the help of a full EM simulator. After this process, final design values are $R_Z = 1.26$, $R_S = 1.2$, $\theta_{C1} = 10^o$, $\theta_{C3} = 6^o$, and $\theta_1 = 53^o$. A pair of vias connecting both ground planes are included within each loop to prevent propagation of waveguide modes. Corresponding layout dimensions are plotted in Fig. 16.

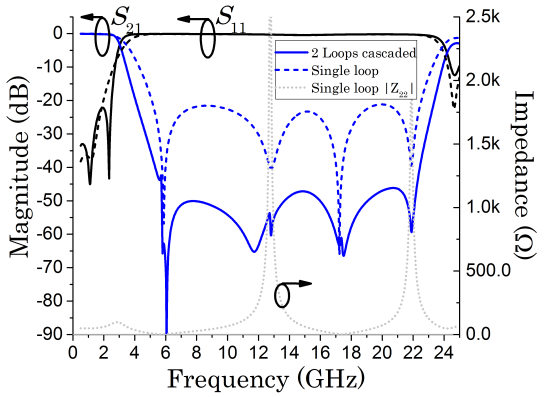

Fig. 17. Basic unit vs. cascaded. Scattering parameters, EM simulated results ($\epsilon_r = 3$)

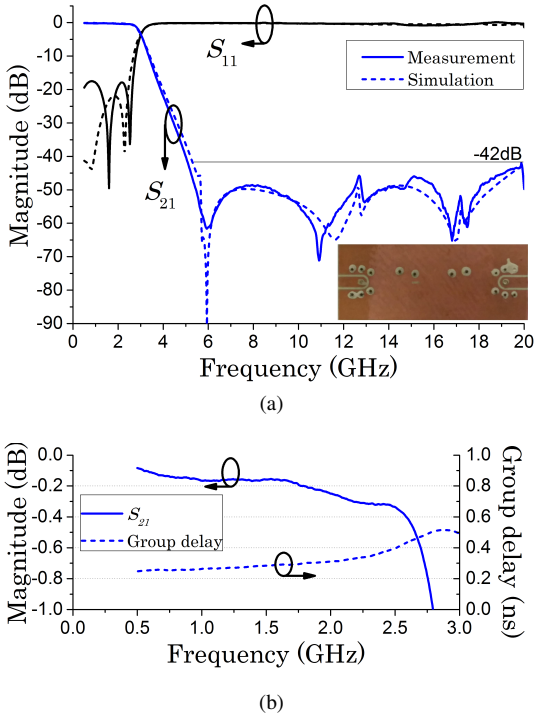

Fig. 18. Measured results vs. EM simulation (including packaging) ($\epsilon_r = 3$) (a) Wideband response. Picture of the fabricated prototype (16.4×6.6 mm^2) (b) Insertion loss and group delay

Simulations for the complete design are plotted in Fig. 17, including the simulation for the optimized single-unit. It can be appreciated how the Z_{in} singularities are matched with the TZ's. Also it can be noticed how the first three TZ's are slightly misplaced with respect to the single unit response. This is produced by the induced coupling between the two loops due to their proximity. The coupling splits TZ's into two, affecting differently depending on the frequency.

A comparison between the full EM simulation and the measured results is shown in Fig. 18. Even though, Z_{in} is not perfectly matched due to the mutual coupling, expected resonances are effectively attenuated without compromising the equal-ripple response. Differences in the location of TP's are due to the effects of the packaging in the simulation.

TABLE I
PERFORMANCE COMPARISON AMONG PUBLISHED FILTERS

	f_c (GHz)	IL (dB) / RL (dB)	Roll-off rate (dB/GHz)	Stopband RJL (dB) / FBW (%)	NCS (λ_g^2)	# Casc. Cells
[2]	2.5	0.45 / 14	24.3	20 / 114.7	0.290 x 0.070	2
[4]	0.5	0.5 / 16.3	95	20 / 140	0.104 x 0.214	1
[5]	3	N/A / 12	42.7	25 / 150	0.310 x 0.240	4
[6]	1.76	0.39 / 14	94.9	23 / 160	0.104 x 0.123	1
[7]	3.12	0.33 / 11.54	30.35	20 / 135.1	0.290 x 0.110	1
[8]	3	0.03 / 20	58.6	25 / 143	0.220 x 0.110	1
[9]	1	0.4 / N/A	21.8	15 / 165.5	0.111 x 0.091	1
[10]	1	0.4 / 20	63	20 / 166.1	0.107 x 0.083	1
[15]	1.26	0.8 / 9	217	20 / 168.5	0.120 x 0.290	1
This work I	2	0.25 / 13.7	20	17 / 139.5	0.070 x 0.070*	1
This work II	3	0.4 / 17.6	18.48	43 / 126	0.161 x 0.070*	2

f_c = Cutoff frequency (3 dB); IL = Insertion Loss; RL = Return Loss;
RJL = Rejection level; FBW = Fractional bandwidth;
NCS = Normalized circuit size; λ_g = Guided wavelength at f_c
(*) Packaging not included

IX. CONCLUSIONS

In this paper a compact, inexpensive, self-packaged low pass structure has been presented, discussing its theoretical principles and demonstrating them through two different examples. A way of improving the rejection in the stopband by cascading two loop-units is also discussed, including the matters related to the interconnection between them. In the first example, a single-loop demonstrating the discussed theoretical principles is covered, followed by a cascaded filter, showing very deep, wide stop-band better with a flat rejection better than 42 dB. Its very low insertion loss makes the filter suitable for clean-up applications.

A performance comparison table (Table I) summarises its main characteristics compared to some other filters found in the literature, showing how this type of filter is capable of matching performance characteristics, with a considerably reduced footprint, also with the advantage of being self-packaged. Covered filters, including packaging, have a footprint of 14.4×7 mm^2 and 16.4×6.6 mm^2, respectively, with very low profile (0.45 mm).

ACKNOWLEDGMENT

The authors would like to thank Dr. Neil Thomson at BSC Filters Ltd.for his support and encouragement throughout this research work.

Francisco Cervera (S'10) received the B.Eng. degree in telecommunications engineering from Universidad Europea de Madrid, Madrid, Spain, in 2007, and the M.Sc. degree in mobile communications from Heriot-Watt University, Edinburgh, U.K., where he is currently working towards the Ph.D.degree. His research interests include miniature, self-packaged, multilayer RF/microwave lters using LCP materials, and integration for wireless communication and radar systems.

Jiasheng Hong (M94-SM05-F12) received the D.Phil. degree in engineering science from the University of Oxford, UK, in 1994. His doctoral dissertation concerned EM theory and applications. In 1994, he joined the University of Birmingham, UK, where he was involved with microwave applications of high temperature superconductors, EM modeling, and circuit optimization. In 2001, he joined the Department of Electrical, Electronic and Computer Engineering, Heriot-Watt University, Edinburgh, UK, and is currently a professor leading a team for research into advanced RF/microwave device technologies. He has authored and coauthored over 200 journal and conference papers, and also two books, Microstrip Filters for RF/Microwave Applications (New York: Wiley, 1st Edition 2001, 2nd Edition 2011) and RF and Microwave Coupled-Line Circuits, Second Edition (Boston: Artech House, 2007). His current interests involve RF/microwave devices, such as antennas and filters, for wireless communications and radar systems, as well as novel material and device technologies including multilayer circuit technologies using package materials such as liquid crystal polymer, RF MEMS, ferroelectric and high temperature superconducting devices.

REFERENCES

[1] R. Gomez-Garcia, M.-A. Sanchez-Soriano, M. Sanchez-Renedo, G. Torregrosa-Penalva, and E. Bronchalo, "Low-pass and bandpass filters with ultra-broad stopband bandwidth based on directional couplers," *IEEE Trans. Microw. Theory Techn.*, vol. 61, no. 12, pp. 4365–4375, Dec 2013.

[2] S. Luo, L. Zhu, and S. Sun, "Stopband-expanded low-pass filters using microstrip coupled-line hairpin units," *IEEE Microw. Wireless Compon. Lett.*, vol. 18, no. 8, pp. 506–508, Aug 2008.

[3] M. Sanchez-Soriano, G. Torregrosa-Penalva, and E. Bronchalo, "Compact filtering structure with four transmission zeros for extended stopband performance," in *European Microwave Conf. (EuMC), 2010*, Sept 2010, pp. 13–16.

[4] V. Velidi and S. Sanyal, "Sharp roll-off lowpass filter with wide stopband using stub-loaded coupled-line hairpin unit," *IEEE Microw. Wireless Compon. Lett.*, vol. 21, no. 6, pp. 301–303, June 2011.

[5] K. Ma and K. Yeo, "Novel low cost compact size planar low pass filters with deep skirt selectivity and wide stopband rejection," in *IEEE MTT-S International Microwave Symp. Dig. (MTT), 2010*, May 2010, pp. 1–1.

[6] M. Hayati, H. Asadbeigi, and A. Sheikhi, "Microstrip lowpass filter with high and wide rejection band," *Electron. Lett.*, vol. 48, no. 19, pp. 1217–1219, September 2012.

[7] M. Hayati, A. Sheikhi, and A. Lotfi, "Compact lowpass filter with wide stopband using modified semi-elliptic and semi-circular microstrip patch resonator," *Electron. Lett.*, vol. 46, no. 22, pp. 1507–1509, October 2010.

[8] M. Mirzaee and B. Virdee, "Realisation of highly compact planar lowpass filter for uwb rfid applications," *Electron. Lett.*, vol. 49, no. 22, pp. 1396–1398, Oct 2013.

[9] J. Wang, H. Cui, and G. Zhang, "Design of compact microstrip lowpass filter with ultra-wide stopband," *Electron. Lett.*, vol. 48, no. 14, pp. 854–856, July 2012.

[10] J. Xu, Y.-X. Ji, W. Wu, and C. Miao, "Design of miniaturized microstrip lpf and wideband bpf with ultra-wide stopband," *IEEE Microw. Wireless Compon. Lett.*, vol. 23, no. 8, pp. 397–399, Aug 2013.

[11] A. Balalem, A. Ali, J. Machac, and A. Omar, "Quasi-elliptic microstrip low-pass filters using an interdigital dgs slot," *IEEE Microw. Wireless Compon. Lett.*, vol. 17, no. 8, pp. 586–588, Aug 2007.

[12] H. Cao, W. Guan, S. He, and L. Yang, "Compact lowpass filter with high selectivity using g-shaped defected microstrip structure," *Progress In Electromagnetics Research Letters*, vol. 33, pp. 55–62, 2012.

[13] M. Kufa and Z. Raida, "Lowpass filter with reduced fractal defected ground structure," *Electron. Lett.*, vol. 49, no. 3, pp. 199–201, Jan 2013.

[14] K. Samanta and I. Robertson, "Characterisation and application of embedded lumped elements in multilayer advanced thick-film multichip-module technology," *IET Microw. Antennas Propag.*, vol. 6, no. 1, pp. 52–59, January 2012.

[15] G. Karimi, A. Lalbakhsh, and H. Siahkamari, "Design of sharp roll-off lowpass filter with ultra wide stopband," *IEEE Microw. Wireless Compon. Lett.*, vol. 23, no. 6, pp. 303–305, June 2013.

[16] J.-M. Muoz-Ferreras and R. Gmez-Garca, "A digital interpretation of frequency-periodic signal-interference microwave passive filters," *IEEE Trans. Microw. Theory Techn.*, vol. 62, no. 11, pp. 2633–2640, Nov 2014.

[17] T. Jensen, V. Zhurbenko, V. Krozer, and P. Meincke, "Coupled transmission lines as impedance transformer," *IEEE Trans. Microw. Theory Techn.*, vol. 55, no. 12, pp. 2957–2965, Dec 2007.

[18] F. Cervera, J. Hong, and N. Thomson, "Development of packaged uwb passive devices using lcp multilayer circuit technology," in *Microwave Integrated Circuits Conf. (EuMIC), 2012 7th European*, Oct 2012, pp. 770–773.